HOSTED BY

National Institute of Oceanography and Fisheries

Egyptian Journal of Aquatic Research

http://ees.elsevier.com/ejar
www.sciencedirect.com

ELSEVIER

National Institute of Oceanography and Fisheries (NIOF)

Egyptian Journal of Aquatic Research

ScienceDirect

FULL LENGTH ARTICLE

Delineating the relationship between chromophoric dissolved organic matter (CDOM) variability and biogeochemical parameters in a shallow continental shelf

CrossMark

Sourav Das [a,*], Sugata Hazra [a], Aneesh A. Lotlikar [b], Isha Das [a], Sandip Giri [a], Abhra Chanda [a], Anirban Akhand [c], Sourav Maity [b], T. Srinivasa Kumar [b]

[a] *School of Oceanographic Studies, Jadavpur University, 188, Raja S. C. Mullick Road, Kolkata 700 032, West Bengal, India*
[b] *Indian National Centre for Ocean Information Services, Kukatpally, Hyderabad, Telangana 500090, India*
[c] *Coastal and Estuarine Environment Research Group, Port and Airport Research Institute, 3-1-1, Nagase, Yokosuka 239-0826, Kanagawa, Japan*

Abstract Absorption coefficient of chromophoric dissolved organic matter (CDOM) at 440 nm [a_{CDOM} (440)], sea surface salinity (SSS), total suspended matter (TSM) and chlorophyll-a (chl-a) were measured during October, 2014 to March, 2015 in the shallow continental shelf waters of the Hugli Estuary, adjacent to West Bengal coast, India. The primary objective of the study was to characterize the relationship between a_{CDOM} (440) and the above mentioned biogeochemical parameters. Upon analyzing the results, we observed that SSS portrayed the best possible relation with a_{CDOM} (440) followed by TSM. Chl-a did not exhibit any statistically significant relationship with a_{CDOM} (440). TSM showed a positive linear relationship with a_{CDOM} (440) ($R^2 = 0.75$) but the relationship did not work at all for the lower end members of TSM values. SSS and a_{CDOM} (440) showed a strong negative relationship throughout the entire data range ($R^2 = 0.96$). In the lower SSS ranges, the relationship showed maximum goodness of fit ($R^2 = 0.99$). Though the goodness of fit between SSS and a_{CDOM} (440) decreased for the higher SSS end members, the relationship was statistically significant all through.

* Corresponding author at: School of Oceanographic Studies, Jadavpur University, Jadavpur, 188 Raja S.C. Mullick Road, Kolkata 700032, West Bengal, India. Fax: +91 33 2414 6242.
E-mail addresses: sourav.biooptics@gmail.com (S. Das), sugata_hazra@yahoo.com (S. Hazra), aneesh@incois.gov.in (A.A. Lotlikar), ishadas2012@gmail.com (I. Das), sandip1989ju@gmail.com (S. Giri), abhrachanda1985@gmail.com (A. Chanda), anirban.akhand@gmail.com (A. Akhand), souravm@incois.gov.in (S. Maity), srinivas@incois.gov.in (T.S. Kumar).
Peer review under responsibility of National Institute of Oceanography and Fisheries.

Introduction

A fraction of Dissolve organic matter (DOM) which exhibits strong absorption of short wavelength radiation and imparts a color to the natural water is termed as chromophoric dissolved organic matter (CDOM) (Coble, 2007). CDOM is found in all natural waters, i.e. marine and fresh water (Kirk, 1994). Generally, CDOM comprises a varying mixture of aliphatic and aromatic polymers that are originated from the degradation of terrestrial and aquatic plant matter (Moran et al., 1999; Raymond and Bauer, 2000).

Marine waters are broadly classified into two categories: Case-I and Case-II (Mobley, 1994). In Case-I waters, remotely sensed ocean color data are principally dependent on the inherent optical properties of the surface water, which in turn, is mostly controlled by phytoplankton, i.e. chlorophyll-a (chl-a) concentration (Ishizaka et al., 2007). However, in Case-II waters, apart from phytoplankton, the optical properties are determined by a variety of other features like total suspended matter (TSM), CDOM and so forth (Branco and Kremer, 2005; Tan et al., 2007). CDOM in Case-II waters poses a problem for accurate chl-a estimation by means of ocean color sensor, since it influences the aquatic light (short wavelength) absorption (Matsuoka et al., 2007). Hence for proper estimation of chl-a from the space (especially in Case-II waters), intensive quantification and compensation of CDOM (Siegel et al., 2005) is required.

The regional assessment of CDOM has gained momentum in recent days mainly in order to correctly analyze the chl-a from remotely sensed data in local scale. In order to address this issue, assessment of CDOM should be downscaled to regional level to account all the possible criteria that are leading to the overestimation of chl-a.

Keeping in view the importance of CDOM measurement discussed so far, several studies have been conducted throughout the globe by means of in-situ sampling (Kowalczuk et al., 2006; Nelson et al., 2004; Sasaki et al., 2008; Takao et al., 2014). In this regard, it is also worth mentioning that in-situ CDOM estimation is more hectic and tricky compared to other hydrological parameters like chl-a, TSS and sea surface salinity (SSS) (Kishino et al., 2005). So, it is convenient to develop an empirical relationship (if found to exist) between CDOM and any other biogeochemical parameters (which is comparatively easier to measure than in-situ CDOM measurement) like SSS, chl-a and TSM for monitoring large scale spatio-temporal CDOM dynamics.

With regard to the above mentioned problem, the present study has been framed in the shallow continental shelf waters situated in the northern part of Bay of Bengal. In this study, we hypothesized that a relationship between the absorption coefficient of CDOM at 440 nm [a_{CDOM} (440)] with each or any of the parameters like SSS, chl-a and TSM exists in this region. The absorption coefficient of CDOM was deliberately chosen for 440 nm since this wavelength lies close to the major absorption band of chlorophyll-a, hence measurement of CDOM at 440 nm can be potentially used directly in remote sensing applications. The first and foremost objective of the present study was to examine and analyze the temporal (monthly) variability of a_{CDOM} (440), SSS, chl-a and TSM throughout the study period by means of in-situ sampling. The second most objective (in accordance with the proposed hypothesis) was to delineate the inter-relationship between a_{CDOM} (440) and the other three parameters.

Materials and methods

Study site

This study has been carried out in the shallow continental shelf waters situated in the northern part of the Bay of Bengal adjoining the coastline of the state of West Bengal, India (Fig. 1). This area receives a huge amount of freshwater discharge from the perennial River Hugli (a distributary of River Ganga) flowing by the megacities of Kolkata and Howrah. Moreover, in the north it is bounded by the world's largest single stretch of mangrove forest, i.e. the Sundarban mangrove ecosystem. Due to a perennial sediment load from the river networks, this region has an extremely shallow and distally elongated continental shelf (Akhand et al., 2013). This region experiences a semidiurnal tide of meso-macro tidal nature (2.5–7 m) and mean current velocities range from 108 cm s^{-1} to 117 cm s^{-1} during high and low tide respectively (De et al., 2011). It is worth to mention, that this study area experiences a steady cloud cover all through the year. Another unique aspect is the variance of SSS exhibited by this region due to the mixing of an enormous freshwater discharge with the typical offshore waters. Even in the post-monsoon season, SSS varied between ∼18 and ∼26 ppt in this region (Das et al., 2015).

The present survey has been conducted at a station (21° 25′ 30″ N; 88° 15′ 30″ E) ∼ 17 km from the shoreline in the shallow continental shelf waters (< 10 m bathymetry) throughout the study period. All the cruises were begun from Frasargunje Fishing Harbour (Lat. 21° 34′ 45″ N; Long. 88° 15′ 05″ E).

Plan of sampling

During the present study period (October, 2014 – March, 2015) a total of twelve (12) sampling surveys were carried out. Two (02) surveys were conducted in each month and three (03) samples were taken in each survey. The entire sampling was accomplished in the daytime during high tide only. In order to provide the immediate ambience a minimum time to attain the equilibrium, the engine was stopped for 15 min before each sampling. Seawater samples were collected using a Niskin sampler (General Oceanics, Inc.) from the water surface (0.25 m below the air–water interface). SSS was analyzed immediately onboard. Samples were transferred into pre-rinsed containers from the Niskin sampler for TSM analysis. For chl-a estimation, water samples were filtered through GF/F (Whatman, 47 mm diameter) filter paper onboard and the filter papers were kept in the liquid nitrogen cylinder until analyzed in the laboratory. CDOM samples are taken according to Sasaki et al. (2005).

Analytical protocol

SSS was measured using a Multikit (WTW Multi 340 i Set; Merck, Germany) fitted with the probe WTW Tetracon 325. In-situ chl-a was measured by means of standard spectrophotometric methods using Shimadzu UV–Visible 1600
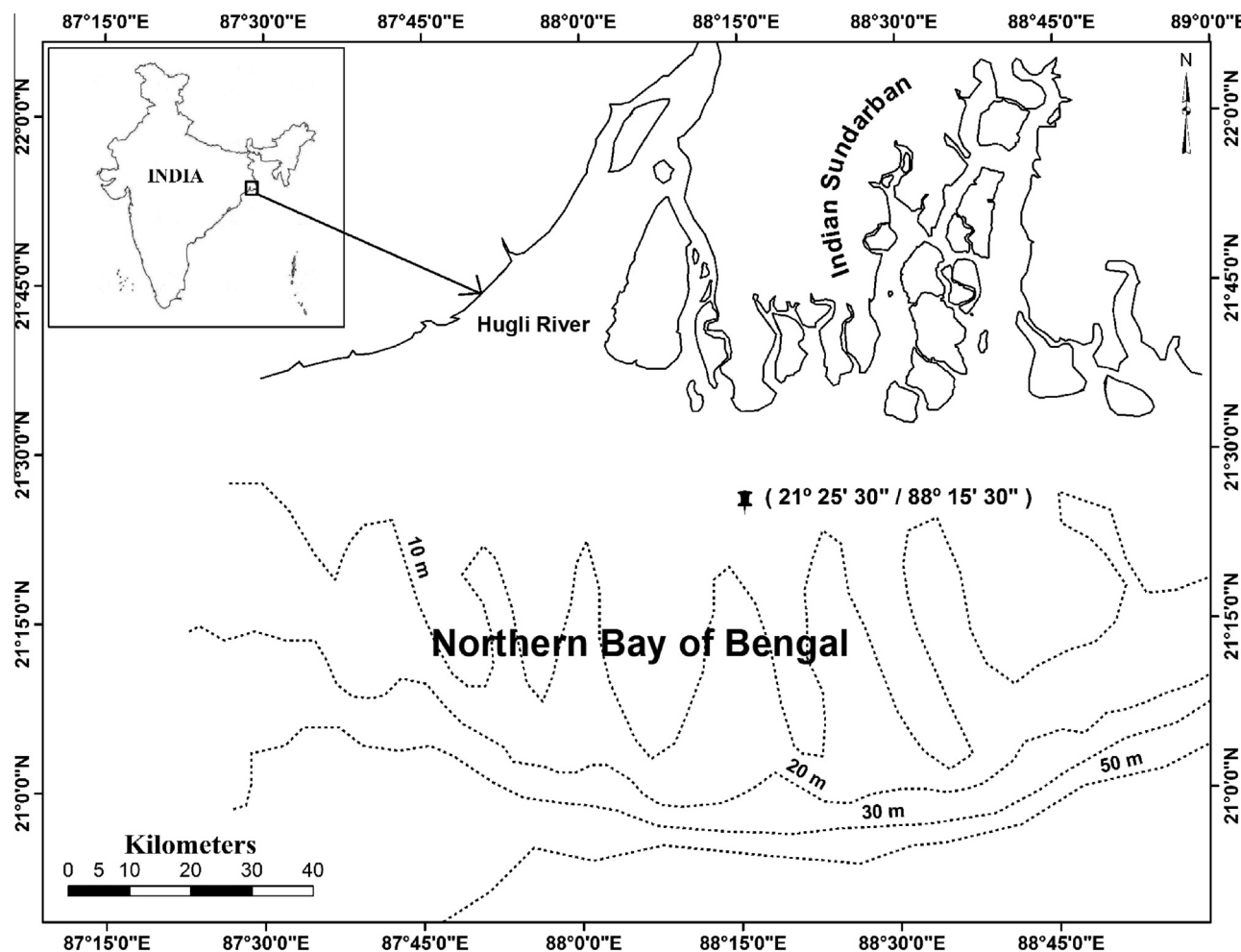
Figure 1 Location of sampling station in the northern part of Bay of Bengal.

double-beam spectrophotometer (Jeffrey and Humphrey, 1975; Parson et al., 1984; Suzuki and Ishimaru, 1990). TSM was analyzed following the procedure outlined by Strickland and Parsons (1972). Absorption coefficient of CDOM was determined following the methods adopted by Sasaki et al. (2005).

CDOM absorption decreases exponentially with increasing wavelength and can be modeled by an exponential decay curve:

$$a(\lambda) = a(\lambda_0)e^{-S(\lambda-\lambda_o)} \qquad (1)$$

where a = Napierian absorption coefficient (m^{-1}), $a(\lambda)$ is the absorption coefficient at wavelength λ (nm), λ_0 is a reference wavelength (nm), and S is referred to as spectral slope. 'S' was calculated by fitting an exponential regression model to the absorption coefficient versus wavelength (see Eq. (1)).

Statistical analysis

The Pearson correlation coefficient (r) was computed between a_{CDOM} (440) and SSS, TSM and chl-a. Linear regression models were tested between a_{CDOM} (440) and SSS, TSM and chl-a using the statistical software package of SPSS (version 16.0). All the graphical representations were prepared using the Grapher 8.

Results

*Status of SSS, TSM and chl-**a** during study period*

October to January marks the post-monsoon season, while February and March happens to be the first half of the pre-monsoon season. Water column depth varied from 7.2 m to 9.1 m during the study period. In February average water depth was the lowest (7.4 ± 0.6 m), whereas in October it was the highest (8.6 ± 0.7 m). SSS was found to increase steadily from October to March (Fig. 2). In October SSS was the lowest (19.6 ± 0.5 psu), whereas by the end of November (25.2 ± 0.8 psu) it increased substantially. In the month of December (26.8 ± 0.5 psu), January (26.3 ± 0.8 psu) and February (26.5 ± 1.1 psu), SSS was more or less constant. TSM concentrations were quite high in the month of October (48.1 ± 2.0 mg l^{-1}) and it decreased in the following months of November (37.4 ± 1.0 mg l^{-1}) and December (24.2 ± 3.6 mg l^{-1}). In the next 3 months, the TSM values were more or less constant (January – 28.3 ± 2.0 mg l^{-1}; February – 23.9 ± 1.1 mg l^{-1}; March – 29.7 ± 3.4 mg l^{-1}) (Fig. 2). Chl-a did not exhibit any such temporal trend. During the month of October (0.35 ± 0.06 mg-m^3), November (0.29 ± 0.05 mg-m^3) and December (0.32 ± 0.07 mg-m^3) its
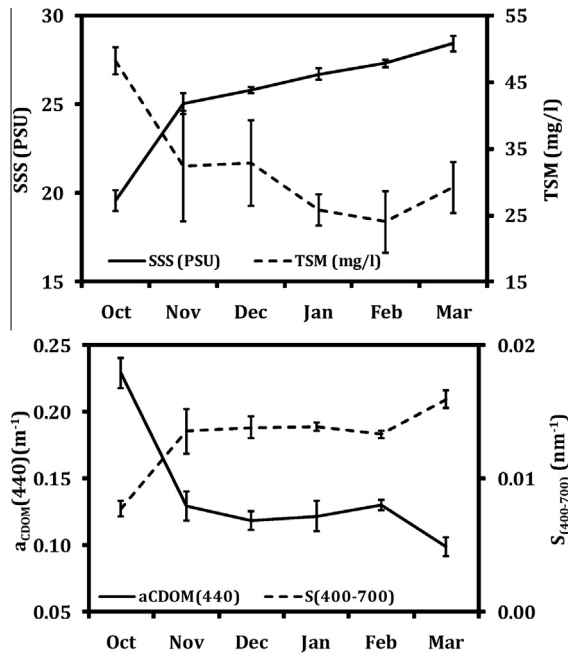
Figure 2 Temporal variability of SSS, TSM, a_{CDOM} (440) and Slope during the study period.

concentration was fairly low. However, during the month of January (1.39 ± 0.05 mg-m^3), the surface chl-*a* concentration was found to increase and the concentration was also quite high in the month of February (1.08 ± 0.09 mg-m^3).

Variability of a_{CDOM} (440) and slope

The a_{CDOM} (440) varied between 0.0862 m^{-1} and 0.2411 m^{-1} during the entire study period, while the spectral slope values ($S_{400-700}$) ranged between 0.0071 and 0.0167 nm^{-1}. During the month of October, a_{CDOM} (440) showed the highest monthly mean value (0.2294 ± 0.0112 m^{-1}) (Fig. 2), whereas, monthly mean $S_{400-700}$ was the lowest (0.0078 nm^{-1}). The monthly mean a_{CDOM} (440) gradually decreased in the following months until December (November – 0.1294 $\pm$ 0.0111 m^{-1}; December – 0.1183 $\pm$ 0.0070 m^{-1}). A marginal increasing signature of a_{CDOM} (440) was also portrayed in the months of January (0.1221 ± 0.0110 m^{-1}) and February (0.1302 ± 0.0037 m^{-1}). The minimum monthly mean a_{CDOM} (440) value was observed during the month of March (0.0987 ± 0.0071 m^{-1}) accompanied by the highest monthly mean $S_{400-700}$ (0.0160 nm^{-1}). An inverse linear relationship was observed throughout the study period between the a_{CDOM} (440) and the $S_{400-700}$ (Fig. 3a). The two parameters were found to be related by the following equation stated below:

$$S_{400-700} = 0.02 - 0.06 \times a_{CDOM}(440) \quad (R^2 = 0.95,$$
$$N = 36, \ p < 0.01) \tag{2}$$

Correlation of a_{CDOM} (440) with SSS, TSM and chl-a

The computed Pearson correlation coefficient (r) between a_{CDOM} (440) and SSS, TSM and chl-*a* depicted reportable linear relation between a_{CDOM} (440) and SSS along with TSM, however, no such relationship was observed between a_{CDOM}

(440) and chl-*a*. The strongest statistically significant correlation (negative) was observed between a_{CDOM} (440) and SSS ($R^2 = 0.96$, $N = 33$, $p < 0.001$) (Fig. 3b) and these two parameters varied with respect to one another based on the equation:

$$a_{CDOM} (440) = 0.51 - 0.015 \times SSS \tag{3}$$

$S_{400-700}$ also showed a significant positive relationship with SSS ($R^2 = 0.93$, $N = 33$, $p < 0.001$) (Fig. 3c) given by the equation:

$$S_{400-700} = 0.0009 \times SSS - 0.01 \tag{4}$$

a_{CDOM} (440) also portrayed a strong correlation with TSM in the entire observed range ($R^2 = 0.62$, $N = 36$, $p < 0.001$) (Fig. 3d), however, the relation was not as strong as observed in case of SSS. The equation portraying the relationship between a_{CDOM} (440) and TSM is:

$$a_{CDOM} (440) = 0.0208 + 0.0037 \times TSM \tag{5}$$

We also separately examined the validity of the regression equation established between a_{CDOM} (440) and SSS throughout the varying range of SSS observed. Upon correlating the a_{CDOM} (440) and SSS within the SSS range of 19–26 psu (Fig. 4a), the highest goodness of fit ($R^2 = 0.99$; $p < 0.01$) was observed. However, the relationship between these two parameters within the SSS range of 24–28 psu showed a sharp drop in R^2 value ($R^2 = 0.61$; $p < 0.01$) (Fig. 4b), though the relationship was statistically significant. Between 27 and 29 psu the goodness of fit of the relationship degraded even more ($R^2 = 0.44$; $p < 0.01$) (Fig. 4c). In the same manner, TSM values were arranged in two separate ranges. The relationship between a_{CDOM} (440) and TSM did not show any statistically significant relationship at all between the TSM range of 16–30 mg l^{-1} ($R^2 = 0.014$; $p = 0.609$) (Fig. 4d). Within the TSM range 30–50 mg l^{-1}, the goodness of fit of the relationship was statistically significant ($R^2 = 0.76$; $p < 0.01$) (Fig. 4e), however, not better than the relationship between a_{CDOM} (440) and SSS comprising the entire range of SSS ($R^2 = 0.96$; $p < 0.01$).

Previous year's trend analysis of a_{CDOM} (440) with respect to SSS variability

This is the first attempt to measure a_{CDOM} (440) in this study region. Das et al. (2015) carried out an exhaustive *in-situ* analysis of several physico-chemical parameters in the post-monsoon seasons between the years 2009–10 and 2013–14 in the same study area. In this study we have utilized the dataset of SSS acquired by Das et al. (2015) along with the observed relationship between a_{CDOM} (440) and SSS found in the present study (Eq. (3)) to develop a trend or assess the variability of a_{CDOM} (440) in the recent past years (Fig. 3e). The composite mean $\pm$ standard deviation (SD) with respect to mean (along with the range) of SSS and derived a_{CDOM} (440) during the post monsoon season of the previous five years is tabulated in Table 1.

Discussion

SSS and TSM were observed to vary temporally during the study period. During the month of October, TSM was quite
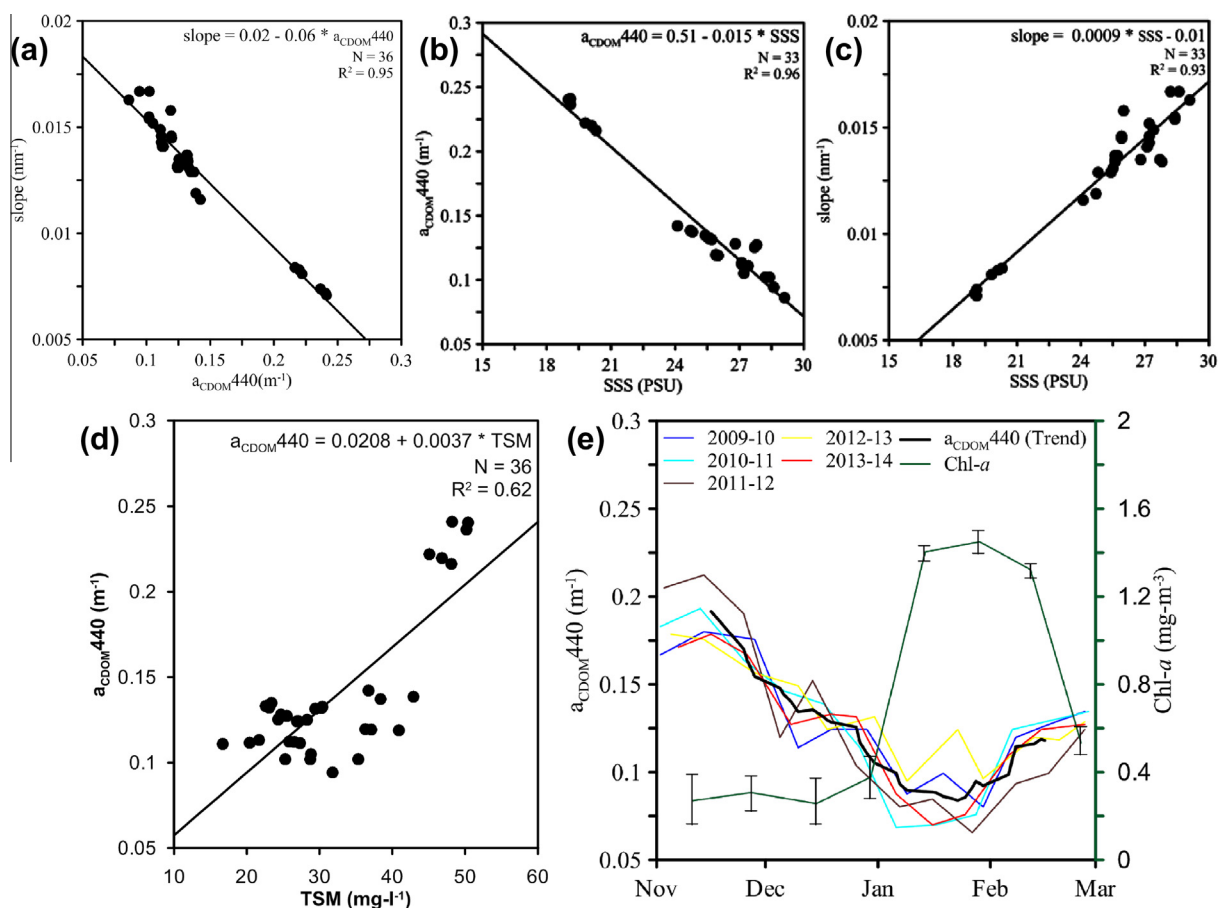
Figure 3 Relationship between (a) a_{CDOM} (440) (m^{-1}) and Slope (nm^{-1}), (b) a_{CDOM} (440) (m^{-1}) and SSS (c) slope and SSS, (d) a_{CDOM} (440) and TSM during the study period (October, 2014 to March, 2015), (e) variability of a_{CDOM} (440) from 2009–10 to 2013–14 (derived from SSS data of Das et al. (2015) by means of Eq. (3)) along with the average chlorophyll-a concentration (measured during October, 2014 to March, 2015) of shallow continental shelf coastal water during post-monsoon.

high accompanied by a substantially low SSS. River Hugli and other associated perennial tributaries bring a huge amount of freshwater during the monsoon season which in turn lowers down the SSS in the northern part of Bay of Bengal (Biswas et al., 2010; Mukhopadhyay et al., 2002). This rainfall driven freshwater discharge carries substantial sediment load as well (Biswas et al., 2004). Due to these two reasons comparatively anomalous values of SSS and TSM were observed during October (i.e. just after the end of monsoon season). On the contrary, in the following months with the advent of post-monsoon season both the freshwater flow and sediment load discharge decreases (Biswas et al., 2004; Mukherjee et al., 2014). This leads to an increasing trend in SSS as observed in this study and a decrease in TSM during the post monsoon months. Chl-a has not shown any such specific trend, however, the marginal increase during the months of January and February is quite justified since phytoplankton blooms were observed to exist near the present study site (i.e. confluence of River Hugli) during the post-monsoon season (Biswas et al., 2010).

The magnitudes of a_{CDOM} (440) observed in the present study are found to have close parity with the a_{CDOM} (440) values reported from several coastal regions (Bowers et al., 2012;

Loisel et al., 2009; Sasaki et al., 2005). The variability of a_{CDOM} (440) is very rarely documented in the surface waters of Bay of Bengal, especially during the post monsoon season. Pandi et al. (2014) while working off the Vishakhapatnam coast (situated in the north western Bay of Bengal) observed a_{CDOM} (440) magnitudes ranging between 0.120 and 0.252 m^{-1} in the month of July (monsoon season). In the same region, Chiranjeevulu et al. (2014) observed a_{CDOM} (350) that ranges 0.322–5.067 m^{-1} during the monsoon season and 0.368–1.934 m^{-1} during the pre monsoon season. It is observed in the present study that a_{CDOM} (440) values were quite high during the end of monsoon and as post monsoon months approached and water flow became lean the values started decreasing. This implies that most of the materials responsible for the increased absorbance of CDOM are principally regulated by the freshwater flow of the Hugli Estuary and mangrove water flushing. Several researchers have shown that the dominant source of CDOM in semi-enclosed coastal seas is mainly derived from terrestrial organic debris transported by the rivers (Coble, 2007; Nelson et al., 1998; Siegel et al., 2002). A marginal increase in a_{CDOM} (440) values was observed during the month of February and incidentally it was accompanied by a small increase in chl-a concentration.
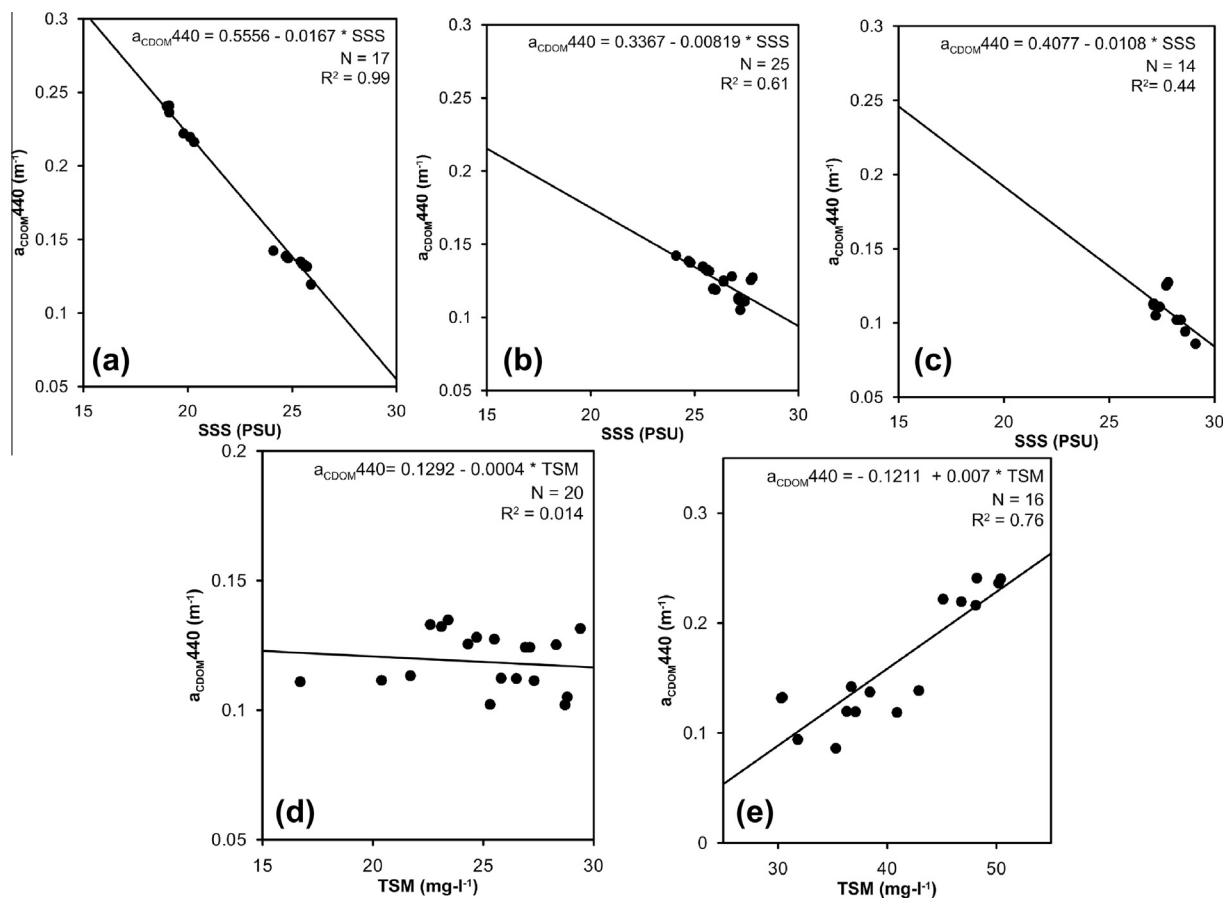
Figure 4 Linear regression relationship between a_{CDOM} (440) with SSS ranges (a) 19–26 psu; (b) 24–28 psu; (c) 27–29 psu; and with TSM ranges (d) 16–30 mg-l^{-1}; and (e) 30–50 mg-l^{-1}.

Table 1 Composite mean ± SD (range) of SSS (Das et al., 2015) and derived a_{CDOM} (440) based on Eq. (3) during the months of November to February of the previous five years.

Year	SSS (psu)	Derived a_{CDOM} (440) (m^{-1})
2009–10	26.2 ± 2.2 (22.6–29.4)	0.1279 ± 0.0324 (0.0802–0.1800)
2010–11	26.1 ± 2.8 (21.7–30.2)	0.1284 ± 0.0414 (0.0685–0.1932)
2011–12	26.2 ± 3.5 (20.4–30.4)	0.1275 ± 0.0507 (0.0655–0.2123)
2012–13	25.8 ± 1.8 (22.7–28.4)	0.1332 ± 0.0271 (0.0949–0.1785)
2013–14	26.3 ± 2.4 (22.7–30.1)	0.1252 ± 0.0356 (0.0699–0.1785)

Similar enhancement of a_{CDOM} (440) values was also observed in other parts of the world followed by an increase in phytoplankton abundance (Sasaki et al., 2005).

The composite mean slope ($S_{400-700}$) observed during the study period was 0.0130 ± 0.0027 nm^{-1}. This observed mean $S_{400-700}$ is quite similar to the global average of 0.0140 nm^{-1} (Del Castillo and Coble, 2000). Pandi et al. (2014) observed a mean $S_{400-700}$ of 0.0143 ± 0.0021 nm^{-1} in the monsoon season. It is a general perception that $S_{400-700}$ and molecular weight of DOM are inversely proportional and that $S_{400-700}$ can be utilized as a proxy of molecular size of DOM (Carder et al., 1989). From the perspective of our study, it can be anticipated that during high freshwater discharge (i.e. when a_{CDOM} (440) values were higher), DOM of higher molecular weight was more prevalent in this region and vice versa.

Among SSS, TSM and chl-a, chl-a did not show any statistically significant relationship with a_{CDOM} (440), as observed by Nelson et al. (1998) and Sasaki et al. (2005). Upon analyzing the entire data set, best possible correlation in the present study was found between a_{CDOM} (440) and SSS (on the basis of the highest goodness of fit) followed by TSM (in this case the goodness of fit was lower). Based on the R^2 values observed between a_{CDOM} (440) and SSS along with TSM for different salinity and TSM ranges, it can again be inferred that SSS is having more significant relationship with a_{CDOM} (440) compared to TSM to assess the variability of a_{CDOM} (440). Thus the framed hypothesis for the present study can be successfully accepted for SSS.

Similar strong relationship between CDOM and SSS was also observed by several workers throughout the globe

Table 2 Relationship observed between SSS and a_{CDOM} (440) in previous studies carried throughout the world.

Study area	Equation	R^2	Reference
Northern Bay of Bengal, India	a_{CDOM} (440) = −0.015 (salinity) + 0.510	0.96	Present study
Northwestern Bay of Bengal, India	a_{CDOM} (440) = −0.011 (salinity) + 0.429	0.77	Pandi et al. (2014)
Arabian Sea (λ = 355 nm)	NA	0.35	Del Castillo and Coble (2000)
Canadian Arctic, Canada	a_{CDOM} (440) = −0.051 (salinity) + 1.61	0.87	Retamal et al. (2007)
Galway Bay, Ireland	a_{CDOM} (440) = −0.029 (salinity) + 1.00	0.71	Goddijn (2007)
Swan River, Australia	a_{CDOM} (440) = −0.109 (salinity) + 4.9	NA	Kostoglidis et al. (2005)
Baltic Sea	a_{CDOM} (440) = −0.171 (salinity) + 1.52	0.88	Kowalczuk et al. (2005)
Conwy, Wales	a_{CDOM} (440) = −0.100 (salinity) + 3.55	0.98	Bowers et al. (2004)
Cape Fear River, USA	a_{CDOM} (440) = −0.169 (salinity) + 6.22	0.96	Kowalczuk et al. (2003)
Clyde Sea, Scotland	a_{CDOM} (440) = −0.082 (salinity) + 2.88	0.99	Binding and Bowers (2003)
Chesapeake Bay, USA	a_{CDOM} (440) = −0.009 (salinity) + 0.42	0.67	Rochelle and Fisher (2002)
Pearl River, China	a_{CDOM} (440) = −0.008 (salinity) + 0.34	0.98	Hong et al. (2005)
St. Lawrence, Canada	a_{CDOM} (440) = −0.031 (salinity) + 1.17	0.99	Nieke et al. (1997)

(as tabulated in Table 2). The present study area lies in the transition zone between a meso-macro tidal estuary and off shore (Akhand et al., 2013), where SSS is mainly regulated by the mixing processes of Hugli River and other distributaries driven freshwater and waters of offshore region. Since most of the CDOM available in this region is allochthonous in nature (i.e. derived from freshwater input), CDOM and SSS are expected to co-vary having a similar pattern. In this regard, Binding and Bowers (2003) pointed out that high river discharge (accompanied by high CDOM concentration) generally leads to a gentler gradient in the relationship between CDOM and SSS. This principle of variability of these two conservative parameters in the estuarine phase might be the main probable reason behind such a strong relationship observed between a_{CDOM} (440) and SSS.

Based on the relationship between a_{CDOM} (440) and SSS (according to Eq. (3)) the a_{CDOM} (440) magnitudes were derived for the past five year's post-monsoon months. The magnitude of derived a_{CDOM} (440) obtained by means of this regression equation was in parity with the measured a_{CDOM} (440) in the present study. The temporal trend of derived a_{CDOM} (440) variability also showed a similar curve throughout the months of November to February. It is worth mentioning that the chl-a concentration which exhibited a marginal increase during the month of January and February was also accompanied by a marginal increase in a_{CDOM} (440) values, however, the increased magnitude was not as high as observed during the end of monsoon (i.e. during October and November) (Fig. 3e). The present observation indicates that allochthonous input of CDOM from the estuaries are the main source of CDOM in this region.

Conclusion

Analyzing all the outcomes from the present study, it can be inferred that in the meso-macro tidal estuary to offshore transition zone situated in the northern part of the Bay of Bengal, SSS and TSM were found to exhibit a linear relationship with the a_{CDOM} (440). Among SSS and TSM, the relationship of a_{CDOM} (440) with TSM was comparatively weaker and it did not work at all for the lower TSM ranges. The linear curve between a_{CDOM} (440) and SSS fitted extremely well in the lower salinity range, while as the salinity increased the relation slightly deteriorated, though remained statistically significant

throughout the entire range of salinity observed during the study period. The derived a_{CDOM} (440) values (2009–10 to 2013–14) depicted similar variability of a_{CDOM} (440) as observed during the present study. This again shows that SSS can be considered as a parameter which can effectively reflect the trend of a_{CDOM} (440) variability with acceptable certainty. However, annual study should be undertaken for complete understanding of the above mentioned relationship. These relationships can be used to developed ecological models and regional algorithms by means of remote sensing in near future.

References

Akhand, A., Chanda, A., Dutta, S., Manna, S., Hazra, S., Mitra, D., Rao, K.H., Dadhwal, V.K., 2013. Characterizing air–sea CO_2 exchange dynamics during winter in the coastal water off the Hugli-Matla estuarine system in the northern Bay of Bengal, India. J. Oceanogr. 69, 687–697.

Binding, C.E., Bowers, D.G., 2003. Measuring the salinity of the Clyde Sea from remotely sensed ocean colour. Estuar. Coast. Shelf Sci. 57, 605–611.

Biswas, H., Dey, M., Ganguly, D., De, T.K., Ghosh, S., Jana, T.K., 2010. Comparative analysis of phytoplankton composition and abundance over a two-decade period at the land-ocean boundary of a tropical mangrove ecosystem. Estuaries Coasts 33, 384–394.

Biswas, H., Mukhopadhyay, S.K., De, T.K., Sen, S., Jana, T.K., 2004. Biogenic controls on the air-water carbon dioxide exchange in the Sundarban mangrove environment, northeast coast of Bay of Bengal, India. Limnol. Oceanogr. 49, 95–101.

Bowers, D.G., Md-Suffian, I., Mitchelson-Jacob, E.G., 2012. Bio-optical properties of east coast Malaysia waters in relation to remote sensing of chlorophyll. Int. J. Remote Sens. 33, 150–169.

Bowers, D.G., Evans, D., Thomas, D.N., Ellis, K., Williams, P.J. le B., 2004. Interpreting the colour of an estuary. Estuar. Coast. Shelf Sci. 59, 13–20.

Branco, A.B., Kremer, J.N., 2005. The relative importance of chlorophyll and colored dissolved organic matter (CDOM) to the prediction of the diffuse attenuation coefficient in shallow estuaries. Estuaries 28, 643–652.

Carder, K.L., Steward, R.G., Harvey, G.R., Ortner, P.B., 1989. Marine humic and fulvic acids: their effects on remote sensing of ocean chlorophyll. Limnol. Oceanogr. 34, 68–81.

Chiranjeevulu, G., Murty, K.N., Sarma, N.S., Kiran, R., Chari, N.V. H.K., Pandi, S.R., Venkatesh, P., Annapurna, C., Nageswara Rao, K., 2014. Colored dissolved organic matter signature and phytoplankton response in a coastal ecosystem during mesoscale cyclonic (cold core) eddy. Mar. Environ. Res. 98, 49–59.

Coble, P.G., 2007. Marine optical biogeochemistry: the chemistry of ocean color. Chem. Rev. 107, 402–418.

Das, S., Chanda, A., Giri, S., Akhand, A., Hazra, S., 2015. Characterizing the influence of tide on the physico-chemical parameters and nutrient variability in the coastal surface water of the northern Bay of Bengal during the winter season. Acta Oceanol. Sin. 34, 102–111.

De, T.K., De, M., Das, S., Chowdhury, C., Ray, R., Jana, T.K., 2011. Phytoplankton abundance in relation to cultural eutrophication at the land-ocean boundary of Sunderbans, NE Coast of Bay of Bengal, India. J. Environ. Stud. Sci. 1, 169–180.

Del Castillo, C.E., Coble, P.G., 2000. Seasonal variability of the colored dissolved organic matter during the 1994–95 NE and SW Monsoons in the Arabian Sea. Deep Sea Res. (Part II) 47, 1563–1579.

Goddijn, L., 2007. PhD Thesis. National University of Ireland, Galway.

Hong, H.S., Wu, J.Y., Shang, S.L., Hu, C.M., 2005. Absorption and fluorescence of chromophoric dissolved organic matter in the Pearl River estuary, South China. Mar. Chem. 97, 78–89.

Ishizaka, J., Siswanto, E., Itoh, T., Murakami, H., Yamaguchi, Y., Horimoto, N., Ishimaru, T., Hashimoto, S., Saino, T., 2007. Verification of vertically generalized production model and estimation of primary production in Sagami Bay, Japan. J. Oceanogr. 63, 517–524.

Jeffrey, S.W., Humphrey, G.F., 1975. New spectrophotometric equations for determining chlorophylls a, b, c1 and c2 in higher plants, algae and natural phytoplankton. Biochem. Physiol. Pflanzen 167, 191–194.

Kirk, J.T.O., 1994. Light and Photosynthesis in Aquatic Ecosystems, 2nd ed. Cambridge University Press.

Kishino, M., Tanaka, A., Ishizaka, J., 2005. Retrieval of Chlorophyll a, suspended solids, and colored dissolved organic matter in Tokyo Bay using ASTER data. Remote Sens. Environ. 99, 66–74.

Kostoglidis, A., Pattiaratchi, C.B., Hamilton, D.P., 2005. CDOM and its contribution to the underwater light climate of a shallow, macrotidal estuary in south-western Australia. Estuar. Coast. Shelf Sci. 63, 469–477.

Kowalczuk, P., Cooper, W.J., Whitehead, R.F., Durako, M.J., Sheldon, W., 2003. Characteristics of CDOM in an organic-rich river and surrounding coastal ocean in the South Atlantic Bight. Aquat. Sci. 65, 384–401.

Kowalczuk, P.A., Stedmon, C., Markager, S., 2006. Modeling absorption by CDOM in the Baltic Sea from season, salinity and chlorophyll. Mar. Chem. 101, 1–11.

Kowalczuk, P., Ston-Egiert, J., Cooper, W.J., Whitehead, R.F., Durako, M.J., 2005. Characterisation of chromophoric dissolved organic matter (CDOM) in the Baltic Sea by excitation emission matrix fluorescence. Mar. Chem. 96, 273–292.

Loisel, H., Mériaux, X., Poteau, a., Artigas, L.F., Lubac, B., Gardel, a., Caillaud, J., Lesourd, S., 2009. Analyze of the inherent optical properties of French Guiana coastal waters for remote sensing applications. J. Coast. Res. 56, 1532–1536.

Matsuoka, A., Huot, Y., Shimada, K., Saitoh, S.I., Babin, M., 2007. Bio-optical characteristics of the western Arctic Ocean: implications for ocean color algorithms. Can. J. Remote Sens. 33, 503–518.

Mobley, C.D., 1994. Light and Water: Radiative Transfer in Natural Waters. Academic press.

Moran, M.A., Sheldon, W.M., Sheldon, J.E., 1999. Biodegradation of riverine dissolved organic carbon in five Estuaries of the Southeastern United States. Estuaries 22, 55–64.

Mukherjee, J., Banerjee, M., Banerjee, A., Roy, M., Ghosh, P.B., Ray, S., 2014. Impact of environmental factors on the carbon dynamics at Hooghly Estuarine Region. J. Ecosyst. 2014, 1–10.

Mukhopadhyay, S.K., Biswas, H., De, T.K., Sen, S., Jana, T.K., 2002. Seasonal effects on the air-water carbon dioxide exchange in the Hooghly estuary, NE coast of Bay of Bengal, India. J. Environ. Monit. 4, 549–552.

Nelson, N.B., Carlson, C.A., Steinberg, D.K., 2004. Production of chromophoric dissolved organic matter by Sargasso Sea microbes. Mar. Chem. 89, 273–287.

Nelson, N.B., Siegel, D.A., Michaels, A.F., 1998. Seasonal dynamics of colored dissolved material in the Sargasso Sea. Deep Sea Res. Part I Oceanogr. Res. Pap. 45, 931–957.

Nieke, B., Reuter, R., Heuermann, R., Wang, H., Babin, M., Therriault, J.C., 1997. Light absorption and fluorescence properties of chromophoric dissolved organic matter (CDOM) in the St. Lawrence estuary (case 2 waters). Cont. Shelf Res. 17, 235–252.

Pandi, S.R., Kiran, R., Sarma, N.S., Srikanth, A.S., Sarma, V.V.S.S., Krishna, M.S., Bandyopadhyay, D., Prasad, V.R., Acharyya, T., Reddy, K.G., 2014. Contrasting phytoplankton community structure and associated light absorption characteristics of the western Bay of Bengal. Ocean Dyn. 64, 89–101.

Parson, T.R., Maita, Y., Lalli, C.M., 1984. A Manual of Chemical and Biological Methods for Seawater Analysis. Pergamon Press, New York, 173.

Raymond, P.A., Bauer, J.E., 2000. Bacterial consumption of DOC during transport through a temperate estuary. Aquat. Microb. Ecol. 22, 1–12.

Retamal, L., Vincent, W.F., Martineau, C., Osburn, C.L., 2007. Comparison of the optical properties of dissolved organic matter in two river-influenced coastal regions of the Canadian Arctic. Estuar. Coast. Shelf Sci. 72, 261–272.

Rochelle-Newall, E.J., Fisher, T.R., 2002. Chromophoric dissolved organic matter and dissolved organic carbon in Chesapeake Bay. Mar. Chem. 77, 23–41.

Sasaki, H., Miyamura, T., Saitoh, S.I., Ishizaka, J., 2005. Seasonal variation of absorption by particles and colored dissolved organic matter (CDOM) in Funka Bay, southwestern Hokkaido, Japan. Estuar. Coast. Shelf Sci. 64, 447–458.

Sasaki, H., Tanaka, A., Iwataki, M., Touke, Y., Siswanto, E., Tan, C. K., Ishizaka, J., 2008. Optical properties of the red tide in Isahaya Bay, southwestern Japan: Influence of chlorophyll a concentration. J. Oceanogr. 64, 511–523.

Siegel, D.A., Maritorena, S., Nelson, N.B., Behrenfeld, M.J., McClain, C.R., 2005. Colored dissolved organic matter and its influence on the satellite-based characterization of the ocean biosphere. Geophys. Res. Lett. 32, 1–4.

Siegel, D.A., Maritorena, S., Nelson, N., 2002. Global distribution and dynamics of colored dissolved and detrital organic materials. J. Geophys. Res. 107, 1–14.

Strickland, J.D.H., Strickland, J.D.H., Parsons, T.R., 1972. A Practical Handbook of Seawater Analysis, 167. Fish. Res. Boar. Can. Bull., p. 311.

Suzuki, R., Ishimaru, T., 1990. An improved method for the determination of phytoplankton chlorophyll using N, N-dimethylformamide. J. Oceanogr. Soc. Jpn. 46, 190–194.

Takao, S., Iida, T., Isada, T., Saitoh, S.-I., Hirata, T., Suzuki, K., 2014. Bio-optical properties during the summer season in the Sea of Okhotsk. Prog. Oceanogr. 126, 233–241.

Tan, C.K., Ishizaka, J., Manda, A., Siswanto, E., Tripathy, S.C., 2007. Assessing post-tsunami effects on ocean colour at eastern Indian Ocean using MODIS Aqua satellite. Int. J. Remote Sens. 28, 3055–3069.